14th International Symposium on Turbulence and Shear Flow Phenomena (TSFP14)
Heidelberg, Germany, July 28–31, 2026

LESS RESTRICTIVE SELF-PRESERVATION SCALINGS FOR NON-CONSTANT SPREADING RATE AXISYMMETRIC JETS

Kenneth Y.-N. Hinh[1], Robert J. Martinuzzi and Craig T. Johansen
Department of Mechanical and Manufacturing Engineering
University of Calgary
2500 University Drive NW Calgary, Alberta T2N 1N4, Canada
kenneth.hinh@ucalgary.ca, rmartinu@ucalgary.ca and johansen@ucalgary.ca

ABSTRACT

Self-preservation scaling is demonstrated in the intermediate region of the axisymmetric incompressible jet using the more general equilibrium similarity framework introduced by Hinh *et al.* (2025). The scaling accounts for the slow-varying local spreading rate of the jet and shows that the second and third velocity moments exhibit self-similarity in the developing region. Particle image velocimetry (PIV) data and direct numerical simulations (DNS) from Nguyen *et al.* (2024) are used to demonstrate self-preservation scalings and to show that self-preservation occurs earlier than in the classical understanding. The scaling is extended to the Reynolds-stress-transport budgets, where the production and turbulence-transport terms collapse under scalings for each component budget. Whereas, for self-preservation, the advection, pressure-gradient, and dissipation terms scale as a group rather than individually. Another group, the difference of the Reynolds normal stresses $(\overline{u^2}-\overline{v^2})/U_m^2$, collapses onto profiles. This group is found to scale independently with b', whereas the individually scaled Reynolds stresses must scale with b' for self-similar profiles. Further analysis shows that the budget of the difference remains unchanged compared with that of the previously studied compressible jet, suggesting a universal underlying structure of jet turbulence.

Introduction

Conventional analyses assume that self-preservation, or equilibrium similarity, occurs in the fully developed far field; when the normalized Reynolds stresses, $\overline{uv}/U_m^2$, $\overline{u^2}/U_m^2$, and $\overline{v^2}/U_m^2$, no longer vary with downstream distance. Although self-preservation analysis has provided insight into the influence of initial conditions and the jet spreading rate, b', (Hussein *et al.*, 1994; George, 1988), the viewpoint where the normalized Reynolds stresses are required to be constant obscures the scaling laws hidden in the turbulent axisymmetric jet. Hinh *et al.* (2025) demonstrated a less restrictive form of self-preservation with the *local* spreading rate, b', a suitable similarity variable. By similarity analysis of the governing equations, various Reynolds stresses, triple correlations, and higher-order turbulence moments can be shown to collapse onto self-similar profiles when normalized by appropriate powers of b'. The scaling has been shown to collapse turbulence moments in a compressible jet, where b' varies with Mach number, and it is hypothesized to also apply to other developing jet flows where b' is non-constant and slowly varying (Hinh *et al.*, 2025). Here, the similarity is revisited to the intermediate region of an incompressible axisymmetric jet. The scaling behavior is compared with that of the compressible jet and with classical far-field behavior. The current analysis shows that the flow development in this region can be consistent with the self-preservation of the governing equations, indicating the presence of an equilibrium state that precedes the classical far-field behavior.

The self-preservation analysis in George (1994) applies equilibrium-similarity techniques to the Reynolds-stress transport equations. Hinh *et al.* (2025) extends this scaling to flows with a local spreading rate, b', where individual Reynolds stresses scale with differing powers of b' depending on the order and direction of the moment. This shows that self-preservation is possible for a wide range of flows, provided that the jet is a slender flow and evolves slowly. The analysis begins with the governing equations of a high-Reynolds-number round jet,

$$\frac{\partial U}{\partial x}+\frac{1}{r}\frac{\partial rV}{\partial r}=0 \tag{1}$$

$$U\frac{\partial U}{\partial x}+V\frac{\partial U}{\partial r}=-\frac{\partial P}{\partial x}+\frac{1}{r}\frac{\partial r\overline{uv}}{\partial r}-\frac{\partial \overline{u^2}}{\partial x} \tag{2}$$

$$U\frac{\partial V}{\partial x}+V\frac{\partial V}{\partial r}=-\frac{\partial P}{\partial r}-\frac{\partial \overline{uv}}{\partial x}+\frac{1}{r}\frac{\partial r\overline{v^2}}{\partial r}. \tag{3}$$

Introducing the following similarity variables,

$$\begin{aligned} &\eta = r/b && P = P_m h(\eta) \\ &U = U_m f(\eta) && \overline{u_i u_j} = r_{ij} R_{ij}(\eta) \\ &V = V_m g(\eta) && \end{aligned} \tag{4}$$

and substituting (4) into (1) - (3) yields the scalings for each term. The scalings are:

$$U_m b' \propto V_m, \tag{5}$$

$$U_m^2 b' \propto U_m^2 b' \propto P_m b' \propto r_{12} \propto r_{11} b', \tag{6}$$

$$U_m^2 b'^2 \propto U_m^2 b'^2 \propto P_m \propto r_{12} b' \propto r_{22}, \tag{7}$$

and corresponding to the individual terms in (1) - (3), respectively. A scaling ambiguity arises since pressure appears to have two scalings - according to $P_m \propto U_m^2$ in (2) and $P_m \propto U_m^2 b'^2$ in (3). Hinh *et al.* (2025) suggests that this can be alleviated by considering the energy exchange between $\overline{u^2}$

and $\overline{v^2}$. Practically, this is performed by substituting the pressure term in (2) with the integrated radial momentum equation, $P_\infty - P = \rho\overline{v^2}$, resulting in,

$$U\frac{\partial U}{\partial x} + V\frac{\partial U}{\partial r} = \frac{1}{r}\frac{\partial r\overline{uv}}{\partial r} - \frac{\partial(\overline{u^2}-\overline{v^2})}{\partial x}, \tag{8}$$

which yield the scaling $(\overline{u^2}-\overline{v^2}) \propto U_m^2$ as a self-preservation constraint. The jet momentum invariant constrains the similarity scaling of the Reynolds stress terms and was found to hold for the compressible jet. Here, it is demonstrated that this scale appears constant across various jet flows. In the intermediate region of the incompressible jet, compatibility with scaling suggests that self-preservation is not restricted to the far downstream region.

In Hinh *et al.* (2025), these equilibrium self-preservation scalings of the mean momentum equation (8) were found to apply to the compressible axisymmetric jet, where b' is attenuated at higher convective Mach numbers, M_c, a phenomenon well studied in compressible mixing layers Bradshaw (1977). When the Reynolds stresses were scaled accordingly, the increasing anisotropy evident at higher Mach numbers was resolved, providing evidence that the mechanism behind the anisotropy of the Reynolds stresses at elevated M_c is due to internal redistribution resulting in equilibrium turbulent energetics satisfying self-preservation. When the self-preservation of high-order moments is accounted for in the Reynolds stress transport (RST) equations or budgets, scaling with powers of b' for self-preservation is required. In the compressible jet data, certain higher-order terms continued to obey self-preservation scaling, whereas others, such as the advection and pressure-gradient terms, did not, and some terms are required to be scaled in groups. It was found that the mean momentum equation obeys the self-preservation scalings, whereas the higher-order terms individually do not. While extensive discussion on the energetics of the RST equations was performed in Hinh *et al.* (2025), it is unclear what observations can be attributed to compressibility effects, and which to the incomplete self-preservation scalings. Further analysis of an incompressible flow exhibiting incomplete self-preservation may provide insight into and ramifications of this class of self-preservation.

The intermediate region has largely been neglected in classical jet literature, as the condition $b' = const.$ as per traditional self-similarity is not satisfied. This region, spanning $10 \lessapprox x/d \lessapprox 30$, is characterized by the reorganization of highly anisotropic structures formed in the near field, which manifest in the scaling of the Reynolds normal stresses that converge toward a traditional self-similar state observed in the far field. These structures, which are sensitive to the jet's initial conditions, advect downstream and influence its subsequent development. Unlike the near region, which has been widely examined in relation to jet instability and noise (Hussain & Zaman, 1981; Petersen & Samet, 1988), and the far region, which has been the focus of self-preservation studies mentioned previously, the intermediate region is underrepresented in the existing literature, considering its application to most practical jet flows. The intermediate region of the jet shows a striking feature: the mean velocity profiles appear to be self-similar much further upstream, at $x/d \approx 15$, and suggest some form of self-preservation within the flow. In contrast, classic self-similarity of the Reynolds normal stresses and higher turbulence moments is observed only further downstream, at $x/d \gtrapprox 30$.

Applying self-preservation principles requires considering the subtleties in determining the scaling of the pressure and pressure-gradient terms. When examining the Reynolds stress budgets, self-preservation of the advection, pressure-gradient correlations, and dissipation terms is not guaranteed individually but can be shown to scale when considered in groups. PIV and DNS datasets are further analyzed to assess the implications of these observations.

1 Jet data

Axisymmetric jet data from experimental PIV and DNS are utilized. The PIV is collected from the facility described in Hinh *et al.* (2025) at Mach numbers M = 0.3 and M = 1.25 at $Re \approx 36000$ and $Re \approx 86000$, respectively. The PIV setup consists of a Photron SA-5 CMOS sensor, a dual-cavity Nd:YLF laser for illumination and seeding from a six-jet Laskin nozzle (TSI 9307-6) with 1 μm Di-Ethyl-Hexyl-Sebacat (DEHS). Image pairs were collected and processed using LaVision DaVis 10.2.0 commercial PIV software. DNS data from the TU Darmstadt Turbulence database for an incompressible turbulent round jet at Re = 3500, see Nguyen *et al.* (2024) and Nguyen & Oberlack (2024).

2 Discussion

Three jet datasets are used to demonstrate the equilibrium self-preservation scaling: subsonic PIV, supersonic M = 1.25 PIV, and incompressible DNS. The influence of the different behavior of b' across the cases is discussed, beginning with mean-field characteristics and Reynolds stresses, and culminating in an analysis of the turbulent energy balance.

2.1 Mean fields

Figure 1 shows the velocity profiles, U/U_m, for the PIV and DNS datasets for $x/d < 25$. The profiles in this region are already self-similar and do not differ between the two jets. The half-width, b, and spreading rate, b' are shown in figure 2. For clarity, the DNS domain has been truncated to show data for $x/d < 60$. Upon closer inspection of both the PIV data and DNS data, it is found that b' is still evolving streamwise for $x/d < 25$. By applying a polynomial curve fit on b to calculate the streamwise rate of change b', it is found that b' is very similar for the subsonic PIV and DNS. The DNS dataset shows that b' approaches an asymptotic value at $x/d = 25$, consistent with classical theory. The M = 1.25 PIV data shows a stronger modification of b' due primarily to M_c, which was previously also described using the self-preservation framework. Figure 3 plots the centerline normalized velocity U_0/U_m, where U_0 is the jet exit velocity. The decreased jet thickness spreading also results in slower velocity decay.

2.2 Reynolds stresses

The Reynolds stresses $\overline{uv}$, $\overline{u^2}$ and $\overline{v^2}$ normalized by the classical scaling, U_m^2, are shown in figure 4. For $x/d < 25$, the Reynolds stresses are observed to be increasing in amplitude. The classical scaling does not lead to a collapse of the profiles. However, concluding that self-preservation is not satisfied is premature. Figure 5 now shows the normalized Reynolds stresses using the self-preservation scalings: $\overline{uv}/U_m^2 b'$, $\overline{u^2}/U_m^2 b'$, and $\overline{v^2}/U_m^2 b'^2$. The scalings $\overline{uv}/U_m^2 b'$ and $\overline{v^2}/U_m^2 b'^2$ are directly from the self-preservation scalings, meanwhile $U_m^2 b'$ was found to best scale $\overline{u^2}$ (Hinh *et al.*, 2025). In contrast to figure 4, the data collapse satisfactorily on a single curve for each Reynolds stress component in Fig 5, show-

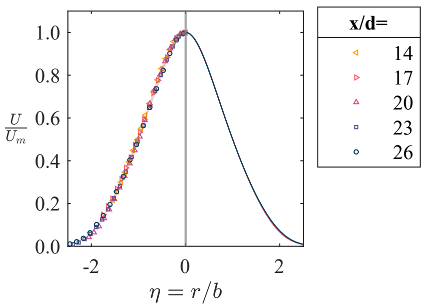

FIGURE 1. Self-similar profiles of U. Subsonic PIV in markers and DNS in markers and lines, respectively.

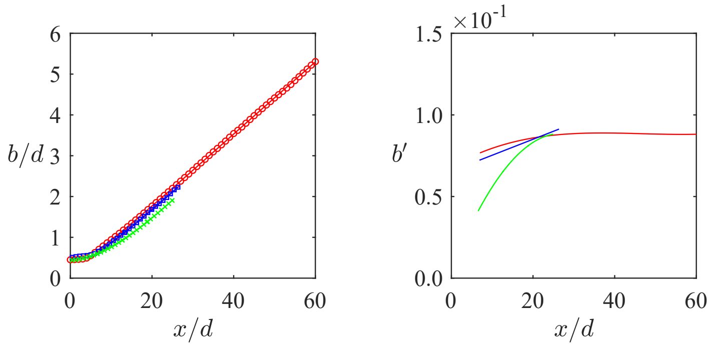

FIGURE 2. Jet half-width thickness, b. Subsonic PIV (□), Mach 1.25 PIV (+) and DNS (○). Spreading rate b' fitted functions in lines of respective colors.

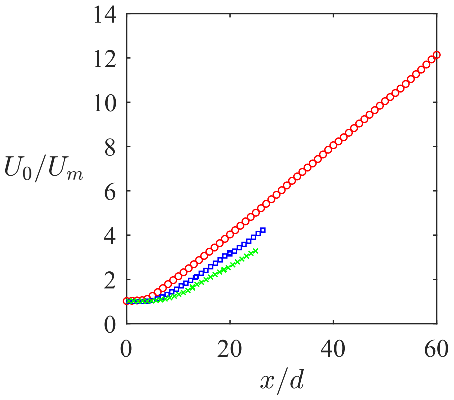

FIGURE 3. Centerline velocity development, U_0/U_m. Subsonic PIV (□), Mach 1.25 PIV (+) and DNS (○).

ing that the applicability of the self-preservation framework applies to the intermediate region.

2.3 Reynolds stress transport balances

The proposed scalings can also be extended to the RST equations, where terms in budgets scale with the form, $b/U_m^3 b'^n$, where n depends on the component direction (Hinh *et al.*, 2025). The terms of RST equations can be collected into the following form, $0 = A_{ij} + T_{ij} + P_{ij} + \Pi_{ij} - \varepsilon_{ij}$, where A_{ij} the advection, T_{ij} the turbulence transport (triple-velocity correlations), P_{ij} the production, Π_{ij} the pressure-velocity gradient correlation and ε_{ij} the dissipation terms. From the framework, self-preservation requires that the $\overline{u^2}$, $\overline{uv}$ and $\overline{v^2}$ balances scale with $b/U_m^3 b'$, $b/U_m^3 b'^2$ and $b/U_m^3 b'^3$, respectively.

To highlight the difference in scaling of the energy balances within the intermediate region of the subsonic PIV and incompressible DNS cases, figures 6 and 7 show the $\overline{uv}$ balance using classical and self-preservation scalings, respectively. As dissipation and pressure-gradient terms are not available from the PIV data, the residual of the balance is plotted. A comparable residual term is also computed for the DNS data set. Figure 6 shows that, in the intermediate region, the budget-term magnitudes increase downstream, indicating a lack of classical self-similarity in both the PIV and DNS data. Using the self-preservation framework in figure 7, the shape and magnitude of each budget term are nearly identical at all axial positions, demonstrating the suitability of the self-preservation framework for this RST component budget. Comparing the PIV and DNS data, the overall structure of the budgets is very similar, with the largest differences occurring in the turbulence transport and advection terms, where the magnitudes are generally larger in the PIV data. The dissipation in the off-diagonal components in the DNS is small, indicating isotropic dissipation and therefore showing that the residual both balances are dominated by the pressure-gradient terms.

Figure 8 plots the $\overline{u^2}$ RST balance with the self-preservation scaling, $b/U_m^3 b'$. It can be observed that the production and turbulence transport terms, which contain the velocity correlations, follow self-preservation scalings. The advection term appears to increase slightly with increasing x/d, an effect more pronounced in the subsonic PIV data. Not shown, the $\overline{v^2}$ balance is found to scale in a similar manner, requiring a different grouping of terms for self-preservation. This behavior in the balance indicates a transition in the redistribution of energy among the terms in the normal-stress balances, with turbulence transport contributing less when b' is lower and advection and pressure-gradient terms playing a larger role. This shows that the structure of energy transport in the normal Reynolds stresses varies with b'.

When considering the transport equations, it can be shown that certain terms, when grouped, satisfy self-preservation. Figure 9 plots groups of terms for each component. For the $\overline{u^2}$ budget, this includes the advection, pressure-gradient, and dissipation terms, and for the $\overline{v^2}$ and $\overline{w^2}$ budgets, this includes the advection and pressure-gradient terms. Apart from near the centerline where the terms are sensitive to gradients, collapse of the profiles is observed. This shows internal energy regulation, with pressure-gradient terms redistributing energy among components and thereby dictating the rate at which the jet develops, which is reflected in the mean field through their effect on the advection terms.

2.4 Reynolds normal stress difference

The proposed scaling of difference $(\overline{u^2} - \overline{v^2})$, which was suggested from the scaling of (8), is investigated next. Figure 10 compares the DNS data to experimental subsonic data. The scaling collapse of the data for both jets confirms the scaling in (8) and emphasizes the importance of accounting for the streamwise pressure development. It appears that the energy exchange of the Reynolds normal stresses is independent of the parameter b'. Using the scale $(\overline{u^2} - \overline{v^2})/U_m^2$, the PIV datasets fall on top of each other while the DNS data appear to collapse on a slightly lower-intensity curve. Although not shown, the subsonic and supersonic PIV data collapse to a similar curve. This discrepancy is perplexing, given the agreement elsewhere, motivating further analysis of the energy budgets.

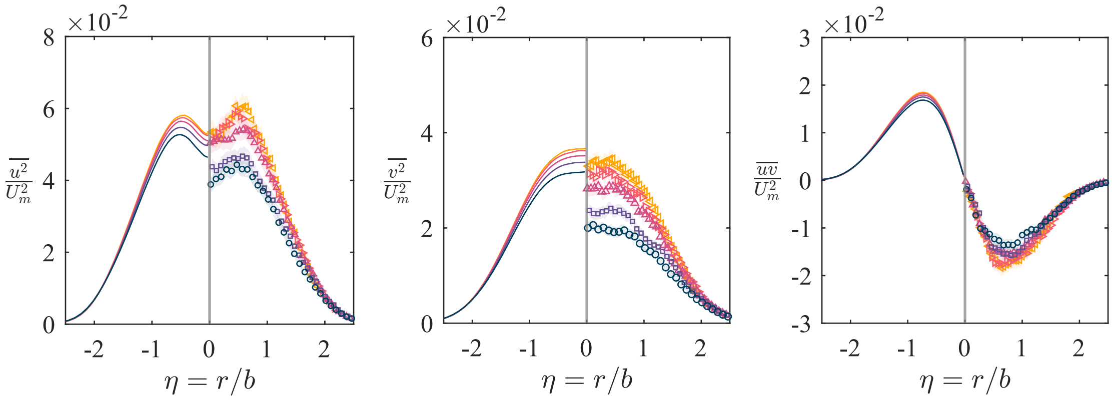

FIGURE 4. Classical scaling of Reynolds stresses. Same legend as figure 1.

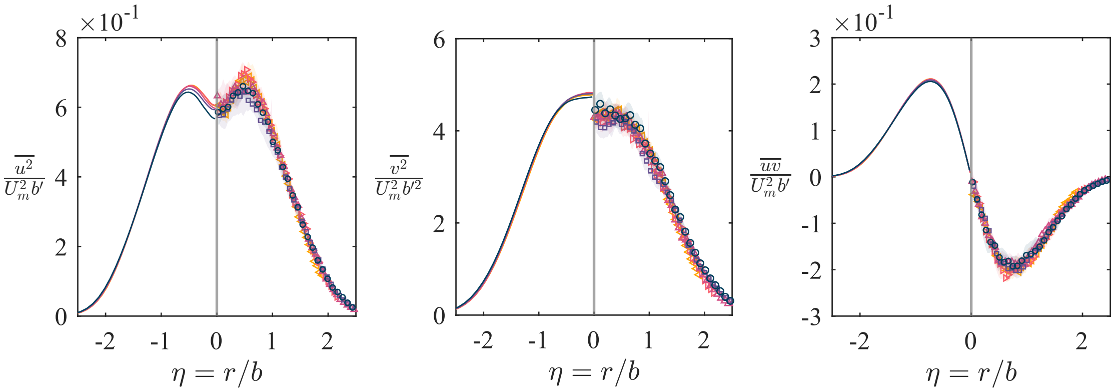

FIGURE 5. Self-preservation scaling of Reynolds stresses with powers of b'. Same legend as figure 1.

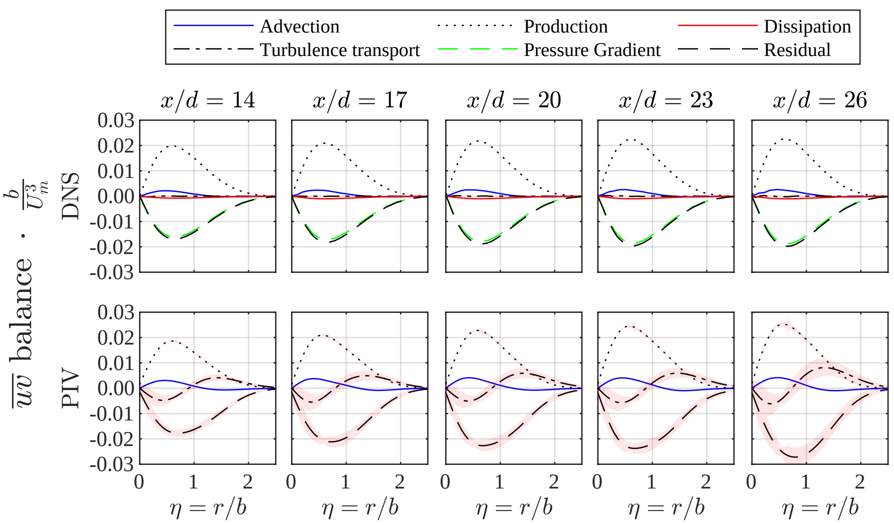

FIGURE 6. Subsonic PIV and DNS $\overline{uv}$ budgets normalized by classical scaling, b/U_m^3.

To demonstrate the scaling behavior of the Reynolds stress difference, figure 11 presents the budget of the Reynolds normal stress difference, $(\overline{u^2} - \overline{v^2})$, normalized by $b/b'U_m^3$, which is the scale determined from the self-preserving framework Hinh *et al.* (2025). This allows for comparison between the DNS and the PIV subsonic and supersonic data. The scaled budgets from both cases agree, with self-similar behavior observed downstream of $x/d \approx 15$ in all cases. For example, the profiles at $x/d = 24$ are shown. In the experimental cases, the pressure-velocity gradient correlation is approximated as the residual of the balance equation, assuming an isotropic dissipation model. Since the DNS simulations, $\varepsilon_{11} - \varepsilon_{22} \approx 0$, this assumption is appropriate. Despite differences in intensity between the PIV and DNS for the profiles of $(\overline{u^2} - \overline{v^2})/U_m^2$, the corresponding terms in the energy balance collapse, suggesting self-preservation. This shows that the process underlying the production, redistribution, and dissipation of energy is similar between the Reynolds normal stresses difference and $\overline{uv}$

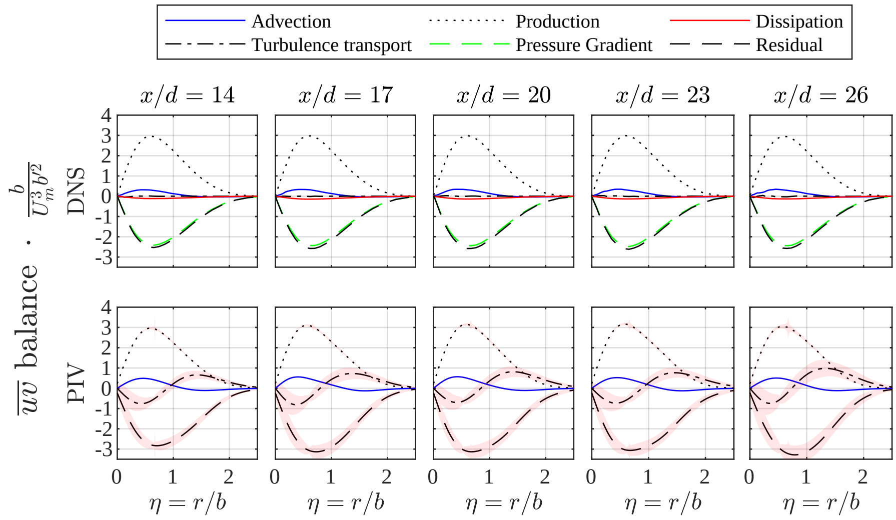

FIGURE 7. Subsonic PIV and DNS $\overline{uv}$ budgets normalized by self-preservation scaling, $b/U_m^3 b'^2$.

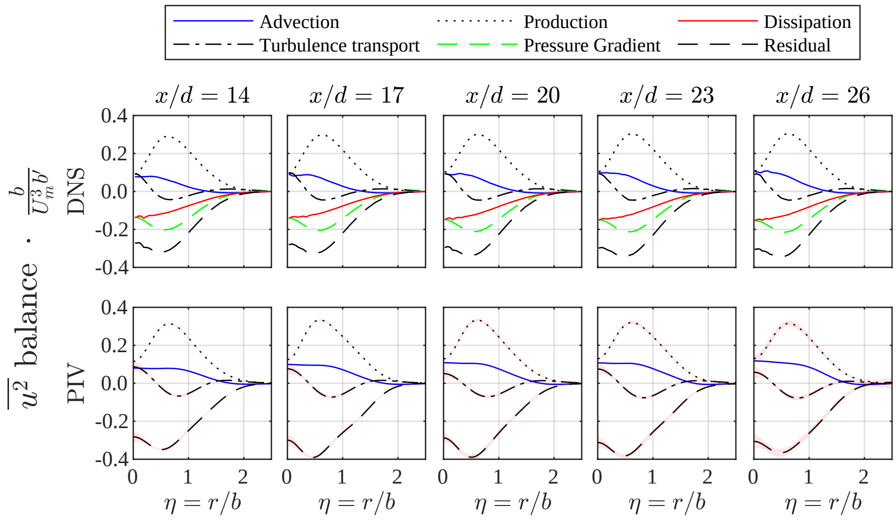

FIGURE 8. Subsonic PIV and DNS $\overline{u^2}$ budgets normalized by self-preservation scaling, $b/U_m^3 b'$.

across various b' values, whereas this was not observed when the normal Reynolds stresses were analyzed individually.

Furthermore, in the normal Reynolds stress balance, a lower spreading rate results in lower production and a corresponding lower pressure-gradient intensity. In supersonic shear layers, it is often hypothesized that the lower pressure-gradient correlation results from physical limitations imposed by the finite speed of sound Pantano & Sarkar (2002). That is, a reduction in the pressure-gradient terms, which require compensation in the remaining balance terms, results in lower production and, thereby, a decrease in the spreading rate. This shows that, despite very different physical mechanisms that reduce the spreading rate, the overall structure of the normal Reynolds stress balance remains unchanged, and, from the perspective of the self-preserving equations, the handling of term scaling is identical.

Conclusion

This study introduces a less restrictive self-preservation framework for axisymmetric jets with non-constant spreading rates, showing that self-preservation emerges much earlier in the jet than traditionally assumed. Using equilibrium similarity scalings based on the local spreading rate b', Reynolds stresses and higher-order turbulence moments in the intermediate region collapse onto universal profiles, resolving the apparent lack of similarity under classical scalings. Experimental and DNS data show that the difference between Reynolds normal stresses, $(\overline{u^2} - \overline{v^2})$, remains invariant with respect to b', indicating a robust underlying turbulent structure that encompasses both compressibility effects and initial conditions. Reynolds stress transport budgets further reveal that, although individual higher-order terms may not scale independently, appropriate groupings of terms exhibit self-preserving behavior, implying that differences in energy redistribution—particularly in pressure-related and turbulence-transport mechanisms—govern the range of jet spreading

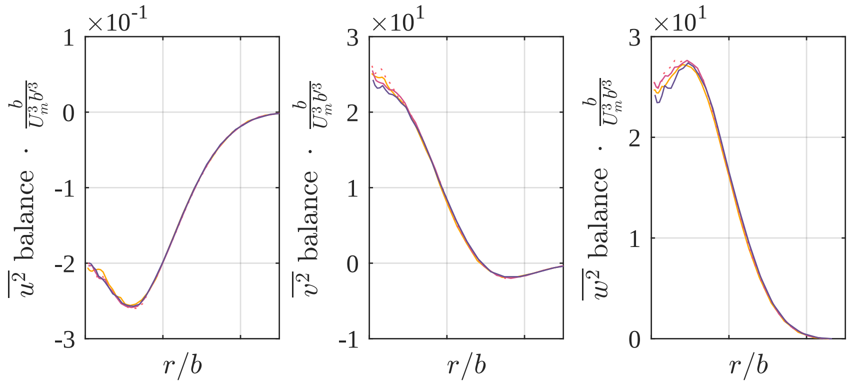

FIGURE 9. Profiles of grouped terms. For the $\overline{u^2}$ budget, the grouped terms comprise the sum of advection, dissipation, and pressure-gradient terms. For the $\overline{v^2}$ and $\overline{w^2}$ budget, the grouped terms comprise the sum of advection and pressure-gradient terms. Same legend as figure 1.

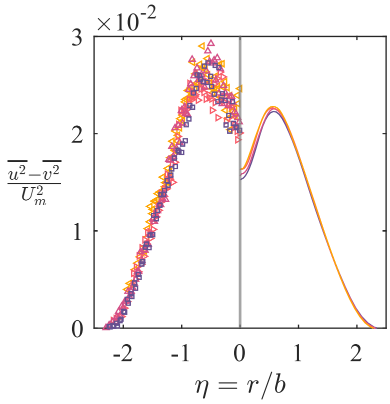

FIGURE 10. Reynolds normal stress difference profiles. Same legend as figure 1.

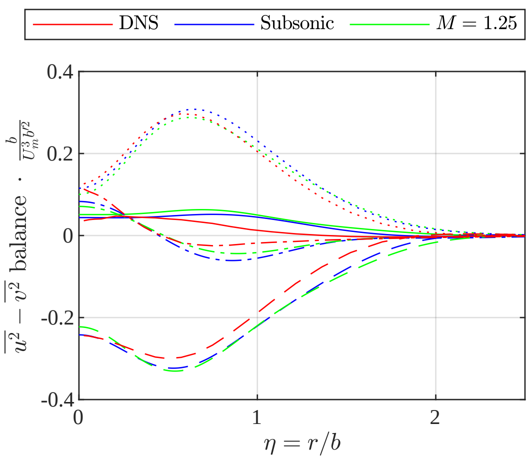

FIGURE 11. Self-preservation scaling of $\overline{u^2} - \overline{v^2}$ balance equation normalized by $b/U_m^3 b'$. Line styles indicating advection (——), production (⋯⋯), turbulence transport (—·—) and pressure gradient (- - - -).

rates. For non-constant b', the scalings suggest that production terms associated with large-scale motions follow the self-preservation framework, whereas the nonlinear terms responsible for energy redistribution must be treated in groups, implying possible physical constraints on redistribution that warrant further study. The scalings also indicate anisotropic behavior, in contrast to classical assumptions of isotropic scaling for pressure-gradient contributions, which can be decomposed into pressure–strain, pressure diffusion, and dissipation. In incompressible flows, continuity requires the trace of the pressure–strain-rate tensor to vanish, which motivated earlier proposals of isotropic scaling in b' (George, 1994). Locally isotropic dissipation models have been widely used in free shear flows. Hussein *et al.* (1994) instead suggests locally axisymmetric behavior, consistent with the present framework in which perpendicular and streamwise components scale differently. The consequences of these scalings for pressure-related terms and turbulence equilibrium from a self-preservation standpoint remain open questions for future work.

REFERENCES

Bradshaw, P. 1977 Compressible Turbulent Shear Layers. *Annual Review of Fluid Mechanics* **9** (1), 33–52.

George, William K. 1988 The Self-Preservation of Turbulent Flows and Its Relation to Initial Conditions and Coherent Structures. *Advances in Turbulence* pp. 39–73.

George, William K. 1994 Some New Ideas on the Similarity of the Turbulent Free Shear Flows. In *Turbulence, Heat and Mass Transfer 1*. Begell House.

Hinh, Kenneth Yi-Nian, Martinuzzi, Robert J. & Johansen, Craig T. 2025 Self-preservation scaling of turbulence in free axisymmetric compressible jets. *Journal of Fluid Mechanics* **1017**, A36.

Hussain, A. K. M. F. & Zaman, K. B. M. Q. 1981 The 'preferred mode' of the axisymmetric jet. *Journal of Fluid Mechanics* **110**, 39–71.

Hussein, Hussein J., Capp, Steven P. & George, William K. 1994 Velocity Measurements in a High-Reynolds-Number, Momentum-Conserving, Axisymmetric, Turbulent Jet. *Journal of Fluid Mechanics* **258**, 31–75.

Nguyen, Cat Tuong & Oberlack, Martin 2024 Analysis of a turbulent round jet based on direct numerical simulation data at large box and high Reynolds number. *Physical Review Fluids* **9** (7), 074608.

Nguyen, Cat Tuong, Oberlack, Martin & TU Darmstadt 2024 DNS data of the turbulent round jet flow at Re=3500.

Pantano, C. & Sarkar, S. 2002 A Study of Compressibility Effects in the High-Speed Turbulent Shear Layer using Direct Simulation. *Journal of Fluid Mechanics* **451**, 329–371.

Petersen, R. A. & Samet, M. M. 1988 On the preferred mode of jet instability. *Journal of Fluid Mechanics* **194**, 153–173.